Available online at www.sciencedirect.com
ScienceDirect
Journal of Photochemistry and Photobiology A: Chemistry 187 (2007) 356–362
Journal of Photochemistry and Photobiology A:Chemistry
www.elsevier.com/locate/jphotochem

Fluorescence quenching inhibition of substituted indoles by neutral and ionized cyclodextrins nanocavities

Raquel E. Galian, Alicia V. Veglia *

Instituto de Investigaciones en Físico Química de Córdoba (INFIQC), Departamento de Química Orgánica, Facultad de Ciencias Químicas, Universidad Nacional de Córdoba, Ciudad Universitaria, 5000 Córdoba, Argentina

Received 2 October 2006; received in revised form 3 November 2006; accepted 6 November 2006
Available online 10 November 2006

Abstract

The effect of cyclodextrins (CDs) in the excited state proton transfer process of indole compounds has been studied by fluorescence quenching, in acid and alkaline media. The quenching efficiency decreases in the presence of CDs in both media indicating a remarkable protection mediated by CD against external quenchers. An interesting non-linear behaviour for the Stern–Volmer plots was observed in basic media. This was interpreted as total inhibition of the quenching process by ionized cyclodextrin. Induced circular dichroism has been used to determine the indole position into the cyclodextrin cavities.

Keywords: Cyclodextrins protection; Excited state proton transfer; Induced quenching; Substituted indole fluorescence; Acid and basic media; Ionized cyclodextrin quenching inhibition

1. Introduction

Tryptophan and its simple derivatives have been used as intrinsic fluorescent probes due to their high dependence on the polarity and rigidity of the surrounding matrix [1]. These properties are also interesting for the development of new electroluminescent materials and artificial photosynthetic devices [2].

The fluorescence quantum yield of simple indoles is independent of pH in the range 3.00–10.00, but is quenched at lower and higher pH [3]. This behaviour is due to two different excited state proton transfer reactions: acid catalyzed protonation of the indole ring and base catalyzed deprotonation of the –NH group.

In other aromatic compounds, it has been demonstrated that the proton induced quenching at moderate acid concentration (pH ∼ 1) proceeds via electrophilic protonation at one of the carbon atoms of the ring in the excited singlet state, leading to proton exchange [4]. Also, it is known that proton induced fluorescence quenching is competitive with proton transfer reaction in the excited state of naphthylamine, naphthols and related compounds [5].

CDs are cyclic oligosaccharides consisting of six (α-CD), seven (β-CD) or eight (γ-CD) units of α-D-glucose linked by α-(1,4) bonds. Among the native CDs derivatives, hydroxypropyl-β-cyclodextrin (HPβCD) has been extensively used due to its higher solubility in aqueous media. The ability of CDs to incorporate guest molecules into their hydrophobic nanocavity (internal diameter/nm: 0.45, 0.70 and 0.85 for α-CD, β-CD and γ-CD, respectively) leading to the formation of host–guest inclusion complexes [6] has permitted their use in different fields [7] like pharmacology, analytical chemistry [8] and synthesis [9]. Additionally, CDs could be used as biological models due to their abilities to modify the photophysical [10] and photochemical properties [11] of the fluorophore included into their cavities. In the literature fluorescence quenching studies using β-cyclodextrin have been reported to characterize the host–guest complexes with 2-acetylnaphthalene [12], acridine [13], dibenzofuran [14] and 1-naphthol [15]. Some examples of the CDs protection towards external quenchers have been published [16]. Low quenching efficiency in the presence of β-CD has been reported for 1-methoxynaphthalene [17] and β-naphthol [18] by proton and iodide ions, respectively. Nevertheless, these results do not agree with those found with carbazole by hydroxide in the presence of CDs [19].

* Corresponding author. Tel.: +54 351 4334170/73; fax: +54 351 4333030.
E-mail address: aveglia@mail.fcq.unc.edu.ar (A.V. Veglia).

1010-6030/$ – see front matter © 2006 Elsevier B.V. All rights reserved.
doi:10.1016/j.jphotochem.2006.11.002

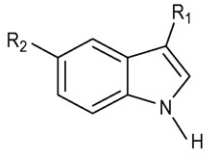

SUBSTRATE	R_1	R_2
3-Methylindole, **3MI**	CH_3	H
3-Indole acetic acid, **3IAA**	CH_2-COOH	H
Trytamine, **T**	CH_2- CH_2-NH_2	H
5-Methoxytryptamine, **5MT**	CH_2- CH_2-NH_2	OCH_3
Melatonin, **M**	CH_2-CH_2-NH-$COCH_3$	OCH_3

Scheme 1. Structures of indole derivatives (S).

Only in few cases the participation of the ionized form of CD has been taken into account [20]. Recently, the formation of the inclusion complex between 1-chloronaphthalene with γ-CD in alkaline solution has been reported [20a]. However, no attention to difference in the efficiency of the quenching process of neutral and ionized cyclodextrin has been considered before [18,19].

The aim of this work is to analyze the effect of cyclodextrins nanocavities in the fluorescence quenching of indole derivatives at pH's where excited stated proton transfer takes place, and particularly to compare the influence of neutral and ionized cyclodextrin. Moreover, from the results of this quenching study and the induced circular dichroism, further knowledge of the orientation of indole compounds inside the cyclodextrins is gained.

Tryptophan metabolites with important implications in the biological area have been chosen for the study (Scheme 1). The electronic characteristic of the substituent at different pHs is considered.

2. Experimental

All the determinations were made at 25.0 ± 0.1 °C, and the temperature of the cell compartment was controlled with a constant temperature circulator. The solutions were not degassed. A solution of 2.40 μM of the substrates at pH 7.0 was used as a reference for the fluorimetric measurements. Buffer solutions were used in order to maintain the pH value. The ionic strength (μ) of all solutions was 0.124 M by adding NaCl. (All other experimental details are in electronic supplementary material (ESM).)

3. Results and discussion

Stern–Volmer plots were used to evaluate the CDs role in the fluorescence quenching by proton and hydroxide. Two cyclodextrin species had to be considered in the basic media (pH 11.00–13.00), the neutral (CD) and the ionized (CD^-), according to the CD pK_a (12.2) [21]. The association constants for the ionized receptor at high pH were determined in order to be compared with the values for neutral CDs.

3.1. Effect of pH and CDs on the fluorescence of indoles

The UV/vis spectra of the substrates (not shown) were not significantly affected by pH changes from 1.00 to 13.00 nor by the presence of β-CD or HPβCD. The molar absorptivity at the maximum around 280.0 nm of the reference solution at pH 7.00 was $(48.4 \pm 0.4) \times 10^2\ cm^{-1}\ M^{-1}$ for **3MI**, $(52.5 \pm 0.5) \times 10^2\ cm^{-1}\ M^{-1}$ for **3IAA**, $(55 \pm 1) \times 10^2\ cm^{-1}\ M^{-1}$ for **T**, $(56.0 \pm 0.5) \times 10^2\ cm^{-1}\ M^{-1}$ for **5MT** and $(56.5 \pm 0.4) \times 10^2\ cm^{-1}\ M^{-1}$ for **M**.

No change was observed in the fluorescence intensity of **3MI** and **M** in the pH range 3.00–11.00. The emission wavelength maximum (λ^{max}) is 370.0 nm (fluorescence quantum yield ($\phi^{pH\ 7} = 0.23$) and 352.0 nm ($\phi^{pH\ 7} = 0.20$) for **3MI** and **M**, respectively (see ESM)). In the case of **3IAA**, the emission intensity at pH 3.00 was lower than at pH 7.00 ($\phi^{pH\ 3}/\phi^{pH\ 7} = 0.46$). The spectrum does not change between pH 5.50 and 10.00, but λ^{max} is 354.0 nm at pH 3.00 and 366.0 nm at pH > 5.50.

On the other hand, the fluorescence of **T** and **5MT** was the same from pH 3.00 to 7.00 with $\lambda^{max} = 355.0$ and 338.5 nm, respectively. In the case of **T**, the fluorescence of the no-ionized substrate was higher than the ionized form ($\phi^{pH\ 10.7}/\phi^{pH\ 7} = 1.23$) with $\lambda^{max} = 364.0$ nm, whereas for **5MT** the opposite effect was observed ($\phi^{pH\ 11}/\phi^{pH\ 7} = 0.90$) with $\lambda^{max} = 359.0$ nm.

In the case of indoles, a simple acid–base equilibrium cannot be attained during the lifetime of the excited state [22]. Therefore, titration curves give the acid–base dissociation constant (K_a) in the ground state [23]. This method was used for **3IAA**, **T** and **5MT** (Table 1).

The acid–base properties in the excited state of aromatic compounds are closely related to the electronic structure and are considerably different from those in the ground state [4,24].

The acidity constant in the excited state (pK_a^*) was determined by the Förster cycle [25] (see frontal face cube in Scheme 2). The values obtained indicate that excitation increases the acidity of the emitting species, as observed in other indole derivatives (Table 1) [22].

For all substrates, an increase in the fluorescence intensity and blue shifts of their maxima were observed with β-CD and HPβCD. These changes are evidence of the inclusion complex formation [26] as observed in other indole derivatives [22,27]. This behaviour was not exhibited in the presence of α-CD, γ-CD or glucose (weight equivalent to 10 mM β-CD) con-

Table 1
Values of pK_a for the free (S) and bound (SCD) substrates in the ground and the excited state

Substrate	pK_a^S	$pK_a^{S^*}$	$(\Delta pK_a)^{S-S^*}$
3IAA	4.48 ± 0.02[a]	3.87 ± 0.05	0.61
T	9.5 ± 0.2	8.4 ± 0.2	1.1
5MT	9.9 ± 0.2	7.7 ± 0.1	2.2
Substrate	pK_a^{SCD}	$pK_a^{SCD^*}$	$(\Delta pK_a)^{SCD-SCD^*}$
3IAA–βCD	4.8 ± 0.1	3.9 ± 0.2	0.9
3IAA–HPβCD	4.63 ± 0.03	3.21 ± 0.05	1.42
T–βCD	9.3 ± 0.2	9.1 ± 0.3	0.2
T–HPβCD	9.1 ± 0.2	9.1 ± 0.2	–
5MT–βCD	9.8 ± 0.2	9.7 ± 0.1	0.1
5MT–HPβCD	9.6 ± 0.3	9.5 ± 0.2	0.1

[a] This value agrees with literature [23].

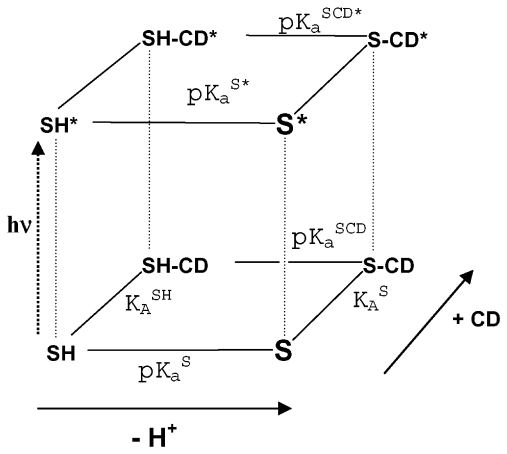

Scheme 2. Representation of acid–base equilibriums in the ground and excited state for the free and complexed substrate with cyclodextrin.

firming that there is some specific interaction with β-CD and HPβCD.

The association constants (K_A) were previously reported by the authors [28] for protic (**3IAA**, **T** and **5MT**) and non-protic substrates (**3MI** and **M**) at pHs where there is no acid or alkaline quenching. The K_A values with 1:1 stoichiometry were higher with HPβCD than with β-CD for all the substrates studied. The fluorescent quantum yield ratios between bound and free substrate (ϕ^{SCD}/ϕ^{S}) were >1. The increase in the quantum yield can be attributed to a decrease in the non-radiative rate constants due to hindered molecular motion for the included substrates. This indicates that the receptor provides a more protected environment for the excited substrate and a lower polarity of the cavity compared with the polarity of water [28].

In the presence of CD, we can represent the system as shown in Scheme 2, where the front and back faces of the cube represent the acid–base equilibriums in the ground and excited state for the free and bound substrate, respectively. The bottom face represents all the equilibriums occurring for the substrate in the ground state when CD is present (thermodynamic cycle), whereas the top face corresponds to the equilibriums taking place in the excited state.

The acidity of the complexes pK_a^{SCD}, lower with **3IAA** and higher with **T** and **5MT**, indicates a better interaction between not ionized substrates and the hydrophobic CDs cavity. The pK_a^* for the complexes ($pK_a^{SCD^*}$) was determined by the Förster cycle. A small increase was obtained in the acidity of the excited state complexes $pK_a^{SCD^*}$ compared to ground state complexes pK_a^{SCD} (Table 1).

3.2. Fluorescence quenching induced by proton

All the substrates showed fluorescence quenching at pH below 3.00 and above 11.00 as previously mentioned in the literature (Fig. 1 is representative) [3,29].

The fluorescence response was measured at different HCl concentrations in the pH range 1.00–3.00. Data were fitted with the Stern–Volmer equation for dynamic quenching (Eq. (1)), where F_0 and F indicate the fluorescence area in the absence

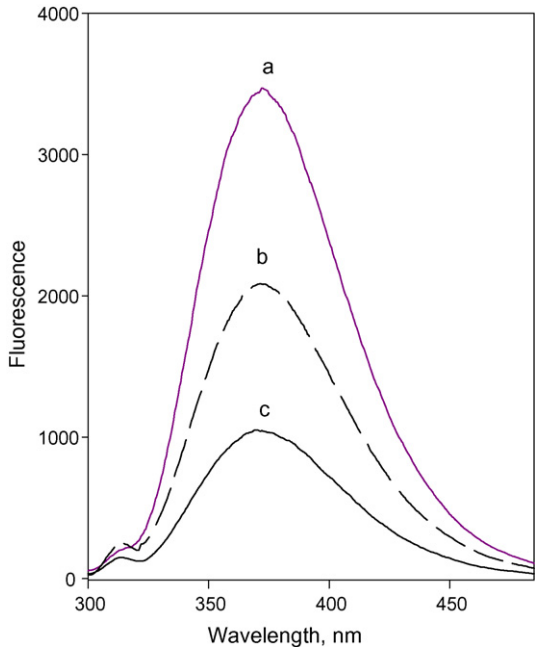

Fig. 1. Fluorescence spectra of **3MI** at different pH's: (a) 7.0, (b) 2.0 and (c) 12.00.

(at pH > 3.00) and in the presence of quencher (proton ions), k_Q represents the bimolecular quenching constant, and τ_0 is the substrate lifetime in the absence of Q. The expression for τ_0 as a function of non-radiative and radiative decay processes is $\tau_0 = (k_{nr} + k_f)^{-1}$. Linear Stern–Volmer plots were obtained and the quenching constant values (K_Q) were determined from the slope of the plots. The K_Q^S are summarized in Table 2.

$$\frac{F_0}{F} = 1 + k_Q\tau_0[Q] = 1 + K_Q^S[Q] \quad (1)$$

Two species accessible to the quencher, the free and bound substrate, were considered for the cyclodextrin effect (0.01 M) in the quenching process. The K_Q^{SCD} was calculated by Eq. (2), where f_i corresponds to the fraction of fluorescence of each species i (S or SCD) at a pH where there is no quenching.

$$\frac{F_0}{F} = \sum_{i=1}^{n}\left\{\frac{f_i}{1 + K_Q^i[Q]}\right\}^{-1} \quad (2)$$

Table 2
Values of Stern–Volmer fluorescence quenching constants by proton (K_{H^+}) for free and bound substrates

Substrate	K_{H^+} (M^{-1})		
	S[a]	S-βCD[b]	S-HPβCD[b]
3MI	115.4[c]	35.1[c]	15.7 ± 0.4
3IAA	34.4[c]	19.77[c]	5.6 ± 0.4
T	33.3 ± 0.3	24.8 ± 0.8	11.6 ± 0.5
5MT	10.5 ± 0.1	6.0 ± 0.2	<0.4
M	48.9 ± 0.3	18.6 ± 0.6	4.6 ± 0.2

[a] Value determined using Eq. (1).
[b] Value determined using Eq. (2).
[c] From Ref. [22].

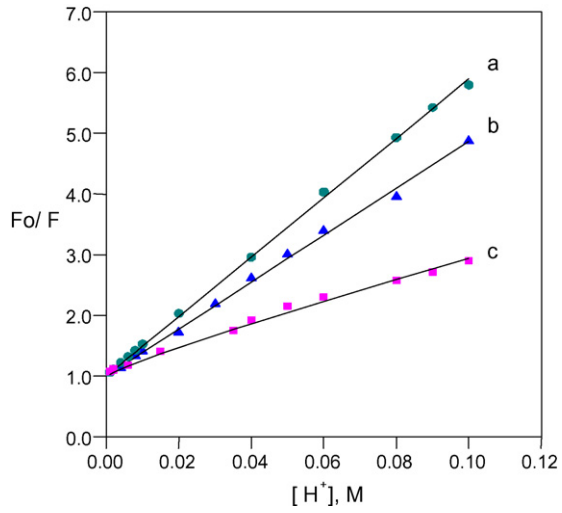

Fig. 2. Stern–Volmer plot for the fluorescence quenching by proton for free **M** (a) and bound **M** with β-CD (b) and HPβCD (c).

The smaller values of K_Q^{SCD} (Table 2) compared to K_Q^S indicate the cyclodextrins protection towards the proton quencher. A diminution around 80% was obtained for HPβCD in the K_Q with respect to the 30–60% with β-CD, consistent with a more hydrophobic environment for the former. The Stern–Volmer plots for **M** are represented in Fig. 2 and similar plots were obtained for the other substrates. A good linearity for the plots using Eqs. (1) and (2) was obtained. Only the dynamic quenching was considered [22].

3.3. Fluorescence quenching in alkaline aqueous solution

The indole fluorescence response in the presence and absence of CDs was analyzed at a pH range 11.00–13.00. A linear behaviour was observed in the absence of CDs. Nevertheless, non-linear plots were obtained in the presence of CDs (Fig. 3 is representative).

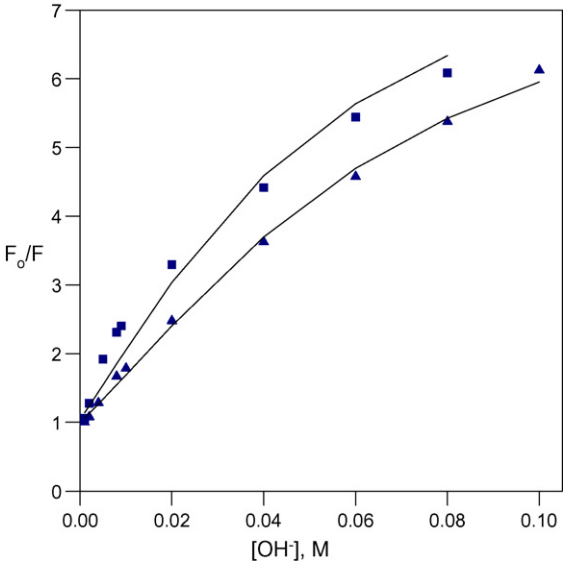

Fig. 3. Stern–Volmer plot for the fluorescence quenching by hydroxide for free and bound **T** with β-CD (■) and HPβCD (▲).

In order to explain this curvature in the presence of receptors, a number of items must be considered: (i) the CD is partially ionized in the pH range studied, therefore, the association between the substrates and the ionized cyclodextrin ($K_A^{SCD^-}$) must be taken into account. Three fluorescent species have to be considered in alkaline media: the free substrate (S), the bound substrate with CD (SCD) and with CD^- (SCD^-); (ii) each of these species have different fluorescence quantum yields and they are represented by ϕ^S, ϕ^{SCD} and ϕ^{SCD^-}; (iii) each of these species have different Stern–Volmer quenching constants and they are represented by K_Q^S, K_Q^{SCD} and $K_A^{SCD^-}$.

The association constants for the substrate with ionized cyclodextrin ($K_A^{SCD^-}$) and the quantum yield ratio between the bound and free substrate (ϕ^{SCD^-}/ϕ^S) were determined at pH 13.00 (where mainly the CD^- is present, Table 3) using the same methodology as previously reported [28]. Fluorescence enhancement indicates absence of quenching by the ionized cyclodextrins.

For the neutral substrates **3MI**, **T**, **5MT**, **M** and for the negative charged **3IAA** at basic media, $K_A^{SCD^-}$ and $\left(\phi^{SCD^-}/\phi^S\right)$ values are similar to those in neutral β-CD (see Table 3, values in parentheses). In the case of HPβCD, no difference is observed in the $K_A^{SCD^-}$ value for **3IAA** (negative charged) in comparison with the values for the neutral HPβCD. However, the $K_A^{SCD^-}$ is lower than for the neutral HPβCD with **3MI**, **T**, **5MT** and **M**. In all cases, higher (ϕ^{SCD^-}/ϕ^S) values are observed for the ionized CD.

Since all the K_A values are $\sim 10^2\ M^{-1}$ (Table 3), these results indicate that the interaction between the indolic substrates and β-CD or HPβCD occurs mainly by the common aromatic moiety, without interaction between the different lateral chain at C-3 (R_1) and the external edge of the β-CD. Similar values of K_A ($\sim 10^2\ M^{-1}$) have been interpreted as preferential aryl inclusion [8c,9c]. Also, the similar values of K_A for **3IAA**$^-$ with neutral and ionized cyclodextrin indicate no repulsion between the deprotonated secondary hydroxyl group and the carboxylate, in agreement with an aromatic interaction between the indolic compounds and the cyclodextrin cavity.

In the case of HPβCD, the higher interaction is found with the neutral receptor ($K_A^{SCD} > K_A^{SCD^-}$). This finding is consistent with some previously reported results with arylic guest and β-CD [20b,20c], but the opposite behaviour was found with a naphthalenic derivative and γ-CD [20a].

In all cases, in the present paper, ionized HPβCD seems to be a better protector of the indole excited state than the neutral receptor (ϕ^{SCD^-}/ϕ^S) > (ϕ^{SCD}/ϕ^S). The opposite effect produced by ionized respect to neutral HPβCD on K_A and ϕ resembles that observed between different cyclodextrins with the same substrate, for example: HPβCD and β-CD with diazepam [8a] or with carbofuran [8b], or between the same cyclodextrin and substituted benzenes [10c] or aromatic carbamates [8b]. The same or the opposite variations in the K_A and ϕ values may be observed by cyclodextrin effect. A general rule to predict these effects cannot be determined, as the static and dynamic interactions are specific to the studied systems and might strongly change at the excited state [7b]. The K_A value depends on several parame-

Table 3
Association constant with ionized cyclodextrins, $K_A^{SCD^-}$ (pH 13.00) and quantum yield ratio between the bound and free substrates (ϕ^{SCD^-}/ϕ^S)[a]

Substrate	β-CD$^-$		HPβCD$^-$	
	K_A ($\times 10^2$ M^{-1})	ϕ^{SCD^-}/ϕ^S	K_A ($\times 10^2$ M^{-1})	ϕ^{SCD^-}/ϕ^S
3MI	0.8 ± 0.5 (1.5 ± 0.3)	1.5 ± 0.2 (1.43 ± 0.1)	0.6 ± 0.2 (1.8 ± 0.1)	3.3 ± 0.4 (2.1 ± 0.2)
3IAA	1.2 ± 0.6 (1.8 ± 0.1)	1.7 ± 0.1 (2.1 ± 0.2)	1.1 ± 0.5 (1.4 ± 0.3)	3.0 ± 0.9 (1.21 ± 0.02)
T	2.4 ± 0.1 (2.8 ± 0.3)	1.40 ± 0.04 (1.25 ± 0.01)	2.0 ± 0.2 (4.9 ± 0.9)	2.41 ± 0.06 (1.33 ± 0.02)
5MT	1.1 ± 0.1 (1.6 ± 0.1)	1.4 ± 0.2 (1.15 ± 0.02)	1.7 ± 0.1 (2.5 ± 0.1)	2.6 ± 0.06 (1.47 ± 0.03)
M	0.8 ± 0.4 (1.1 ± 0.2)	n.d.[b] (1.19 ± 0.03)	0.68 ± 0.03 (1.51 ± 0.07)	3.01 ± 0.07 (1.48 ± 0.03)

[a] Substrate concentration 2.40 μM, cyclodextrin concentration 0–10 mM. For comparison purposes, the K_A^{SCD} values for neutral CDs are given in parentheses [28].
[b] Small changes in fluorescence areas to determine the association values.

ters like H-bonding, hydrophobic and van der Waals forces, size and shape of the guest relative to the host cavity. Meanwhile, the ϕ value is related with the rates of the radiative and no-radiative transitions for the excited state, molecular restriction and elimination of water molecules of the complex substrate [10c].

In the absence of CDs, the values of K_Q were calculated from Eq. (1) (Table 4). These values for the substrates with substitution at the 5-position of the indolic ring (**M** and **5MT**) are smaller than for the others.

The excited state proton transfer reaction of indole and similar structures in basic media has been studied using picosecond time-resolved techniques. The process is diffusion controlled, $k_Q = 26.38 \times 10^9$ M^{-1} s^{-1} for indole at 26 °C [30]. Theoretical values of K_Q, calculated (Eq. (1)) using k_0 and τ_0 from the literature [22] are in the same order as the experimental values reported in Table 4.

In presence of CDs, the molar fraction of the species accessible to the quencher (S, SCD and SCD$^-$) changes when the concentration of hydroxide increases. Therefore, in order to find the function that relates the ratio F_0/F to the hydroxide concentration, some equations were considered (see ESM) to give the following Eq. (3):

$$\frac{F_0}{F} = \left\{ \left(\frac{1}{1 + K_Q^S[Q]} \right) \left(\frac{X_Q^S}{X^S} \right) f^S + \left[\left(\frac{1}{1 + K_Q^{SCD}[Q]} \right) \times \left(\frac{X_Q^{SCD}}{X^{SCD}} \right) + \left(\frac{\phi_Q^{SCD^-}}{\phi^{SCD}} \right) \left(\frac{X_Q^{SCD^-}}{X^{SCD}} \right) \right] f^{SCD} \right\}^{-1} \quad (3)$$

A detailed treatment of the data is described for **T** (ESM). The constant value for the quantum yield ratio $\phi_Q^{SCD^-}/\phi^{SCD}$ with the increasing hydroxide concentration indicates that the bimolecular quenching constant for the ionized cyclodextrin $k_Q^{SCD^-}$ is practically zero.

The average $\phi_Q^{SCD^-}/\phi^{SCD}$ values obtained following the same procedure as before for all the substrates are informed in Table 4.

The protection of cyclodextrin nanocavities to the external quencher like hydroxide was observed for both CDs but was higher for HPβCD. Nevertheless, the best effect obtained was with ionized cyclodextrin nanocavities that indicate that the fraction of the substrate bond to CD$^-$ is not accessible to the quencher producing the downward curvature shown (Fig. 3) [1d].

3.4. Structure of host–guest complexes

The orientation of the substrates into the cavity seems to play a key role in the excited state proton transfer process. Thus, the fact that the prototropic process is favoured or not, depends on the CD-imposed microenvironment to the guest molecule and the orientation of protonation/deprotonation centres.

The cyclodextrin effect in excited state proton transfer reactions previously reported for other aromatic compounds, indicates a decrease in the efficiency of proton and hydroxide induced quenching for 1-methoxynaphthalene [17], 2-naphthols [18] and 2-naphthylamine [31], and an increase in the deprotonation rate for carbazole [19,31].

In the cases of naphthalenes, the protection of protonation/deprotonation centres included into cyclodextrin were

Table 4
Stern–Volmer fluorescence quenching constant $\left(K_Q^{OH^-}\right)$ by hydroxide and (ϕ^{SCD^-}/ϕ^{SCD})[a] values

Substrate	$K_Q^{OH^-}$ (M^{-1})			(ϕ^{SCD^-}/ϕ^{SCD})[a]	
	S[b]	S-βCD[c]	S-HPβCD[c]	S-βCD$^-$	S-HPβCD$^-$
3MI	70 ± 1	21 ± 5	37 ± 2	0.20 ± 0.02	0.341 ± 0.09
3IAA	60.0 ± 0.5	27 ± 4	17 ± 3	0.15 ± 0.02	0.182
M	39.0 ± 0.4	30 ± 5	20 ± 2	0.24 ± 0.01	0.38 ± 0.01
T	71.1 ± 0.5	42 ± 7	36 ± 1	0.16 ± 0.01	0.181 ± 0.08
5MT	39.3 ± 0.3	28 ± 3	12 ± 2	0.26 ± 0.01	0.30 ± 0.03

[a] Average value, independent of hydroxide concentration as indicated in the text, therefore $K_Q^{SCD^-} \approx 0$.
[b] Value obtained from Eq. (1).
[c] See text for a detailed explanation.

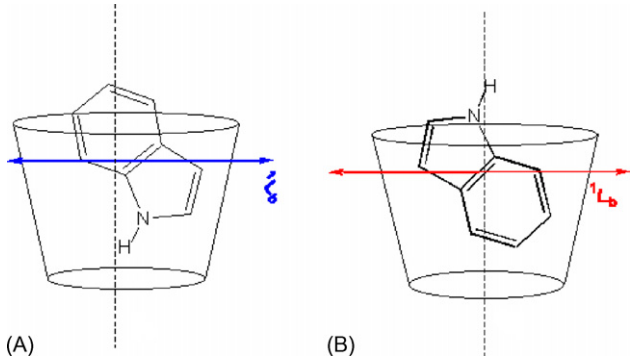

Scheme 3. Complex structures of indole derivatives proposed considering the quenching fluorescence results. 'A' indicates that positions C-2, C-7 and –NH are included into the cavity and 'B' indicates that positions C-4, C-7 are included into the cavity.

proposed to be responsible for the proton transfer quenching decrease [17–19].

On the other hand, for the proton transfer quenching increase with carbazole [19,31] in the presence of β- or γ-CD, it was suggested that the polar group NH (carbazole) was peeping through the bulk water phase, and the aromatic rings remained within the less polar CD cavity. Furthermore, a cyclodextrin cooperative effect involving a flip-flop hydrogen bonding between the CDs hydroxyl and the –NH group was proposed.

Induced circular dichroism spectra (ICD) provide information about the orientation of the guest molecule into the CDs cavities. The absorption spectrum of indole derivatives above 260 nm is a superposition of the two bands ^1L_a ($\lambda_{max} \approx 270$ nm) and ^1L_b ($\lambda_{max} \approx 280$–290 nm). Fluorescence of indoles in polar solvents can occur from both the ^1L_a and ^1L_b states although emission only from the ^1L_a has been observed upon excitation at 286 nm of the $^1L_b \leftarrow {}^1A$ band of indole or tryptophan in propylene glycol [1a].

In the absorption region, the ICD spectra (not shown) of **M** and **T** at pH 7.00 (as a model of neutral and ionized indolic compound) have a negative Cotton effect, with a peak at 280.3 and 281.3 nm for **M** and a peak at 283.5 nm for **T** in the presence of 10 mM of β-CD or HPβCD, respectively, corresponding to the ^1L_b transition.

The directions of the transition moments of indoles have been previously determined [32a]. The negative Cotton effect observed in ICD [32b] indicates that the ^1L_b transition is perpendicular to the CD symmetry axis from Kirkwood–Tinoco rules [32c]. Two orientations of the substrates into the cyclodextrin cavity have been proposed, taking into account the carbon atoms involved in the electrophilic attack at indolic ring (C-4 and C-2) by proton and the –NH indolic group deprotonation by hydroxide (Scheme 3).

If the substrates were included by the benzilic ring (structure B), the C-4 at the indolic ring could be protected by the CD environment and the –NH group could form a hydrogen bond with the secondary hydroxyl group of the bigger cyclodextrin side. A similar structure has been proposed for carbazoles in the presence of cyclodextrin to explain the increase in the deprotonation rate towards –NH group. In alkaline media, where CD is ionized, a stronger hydrogen bond could take place. However, in this study we have observed a quenching protection in the presence of neutral CD and ionized CD^-; consistently, structure B cannot be considered. Therefore, structure A is proposed where the C-2 and –NH are included into the cavity. In this case, quenching by proton can occur mainly at C-4 and the –NH deprotonation process is less accessible by hydroxide in the presence of neutral CD. Also, this is practically inaccessible with ionized CD^-, due to an electrostatic barrier from the secondary ionized hydroxyl of the cyclodextrin. Also, structure A is consistent with the idea of the interaction of aromatic guests with cyclodextrins may be accounted for in terms not only of the hydrophobic effect but the dipole–dipole interaction between the host and the guest [6b].

In addition, the different orientation of naphthalene and indole derivatives (two aromatic rings) inside the CD cavity with respect to carbazoles (three aromatic rings) is consistent with the smaller molecular size of the two first compounds resulting in more deeply inclusion complexes.

No more insight was provided by H NMR studies. The shift of the signal in presence of receptor with respect to the signal of the substrate or the cyclodextrin alone ($\Delta\delta$) is used as probe of inclusion. The experiments performed with the maxima cyclodextrin concentration or in the best condition only shown $\Delta\delta_{max} = 0.01$ ppm. These small changes are proof of inclusion but do not permit the K_A determination or the complex structure determination (see ESM).

4. Conclusions

The fluorescence quantum yield of the indole derivatives is sensible to the pH (<3.0 and >11.0) and to the presence of cyclodextrin nanocavities. The acid catalyzed protonation of the indole ring and base catalyzed deprotonation of the –NH group are responsible for the proton induced quenching process. An important effect of CDs in the excited stated proton reactions in acid and basic media has been observed. The Stern–Volmer quenching constants showed smaller values in the presence of the receptors indicating the protection of the excited stated.

The non-linear behaviour exhibited in an alkaline medium in the presence of the receptors was explained by the co-existence of three species accessible to the quencher, the free substrate and the bound substrate with neutral and ionized cyclodextrin. The changes in those fractions as the pH increases produce a curvature in the Stern–Volmer plots. Interestingly, a partial protection in the presence of a neutral CD was observed while the fraction bound with the ionized CD was inaccessible to the quencher.

The ^1L_b excited electronic state of the indoles was perpendicular to the cyclodextrin axis as demonstrated by ICD. The C-2 and –NH group are partially included into the receptor nanocavity and consequently protected from external quenchers.

Acknowledgements

This research was supported in part by Consejo Nacional de Investigaciones Científicas y Técnicas (CONICET); Agencia Córdoba Ciencia, Córdoba, Argentina; Secretaría de Cien-

cia y Tecnología de la Universidad Nacional de Córdoba (SECyT-UNC); Agencia Nacional de Promoción Científica y Tecnológica (FONCYT). REG was a grateful recipient of a fellowship from CONICET. We thank very much Prof. Dr. Rita H. de Rossi for revisions, comments and suggestions.

Appendix A. Supplementary data

Supplementary data associated with this article can be found, in the online version, at doi:10.1016/j.jphotochem.2006.11.002.

References

[1] (a) D. Creed, Photochem. Photobiol. 39 (1984) 537;
(b) J.R. Lakowicz, I. Gryczynski, H.C. Cheung, C.-K. Wang, M.L. Johonson, N. Joshi, Biochemistry 27 (1988) 9149;
(c) J.W. Petrich, J.W. Longworth, G.R. Leming, Biochemistry 26 (1987) 2711;
(d) J.R. Lakowicz, Principles of Fluorescence Spectroscopy, 2nd ed., Kluwer Academic/Plenum Publishers, New York, 1999, p. 248.
[2] S.K. Pal, T. Bhattacharya, T. Misra, R.D. Saini, T. Ganguly, J. Phys. Chem. A 107 (2003) 10243.
[3] (a) A. White, Biochem. J. 71 (1959) 217;
(b) S.S. Lehrer, J. Am. Chem. Soc. 92 (1970) 3459.
[4] H. Shizuka, S. Tobita, J. Am. Chem. Soc. 104 (1982) 6919.
[5] H. Shizuka, Acc. Chem. Res. 18 (1985) 141.
[6] (a) M.L. Bender, M. Komiyama, Cyclodextrin Chemistry, Springer-Verlag, Berlin, Heidelberg, 1978;
(b) M.V. Rekharasky, Y. Inoue, Chem. Rev. 98 (1998) 1875.
[7] (a) R. Hedges, Chem. Rev. 98 (1998) 2035;
(b) A. Douhal, Chem. Rev. 104 (2004) 1955.
[8] (a) R.P. Frankewich, K.N. Thimmaiah, W.L. Hinze, Anal. Chem. 63 (1991) 2924;
(b) N.L. Pacioni, A.V. Veglia, Anal. Chim. Acta 488 (2003) 193;
(c) N.L. Pacioni, A.V. Veglia, Anal. Chim. Acta 583 (2007) 63.
[9] (a) A.V. Veglia, R.H. de Rossi, J. Org. Chem. 53 (1988) 5281;
(b) A.V. Veglia, R.H. de Rossi, J. Org. Chem. 58 (1993) 4941;
(c) A.V. Veglia, R.H. de Rossi, Can. J. Chem. 78 (2000) 233.
[10] (a) V. Balzani, F. Scandola, Supramolecular Photochemistry, Ellis Horwood, Great Britain, 1991;
(b) P. Bortolus, S. Monti, Adv. Photochem. 21 (1996) 1;
(c) K. Kalyanasundaram, Photochemistry in Microheterogeneous Systems, Academic Press, Orlando, FL, 1978.
[11] (a) P.P. Levin, Y.N. Malkin, V.A. Kuzmin, Chem. Phys. Lett. 175 (1990) 74;
(b) S. Sortino, J.C. Scaiano, G. De Guidi, S. Monti, Photochem. Photobiol. 70 (1999) 549;
(c) S. Monti, S. Sortino, Chem. Soc. Rev. 31 (2002) 287.
[12] L.K. Fraiji, D.M. Hayes, T.C. Werner, J. Chem. Educ. 69 (1992) 424.
[13] J.M. Schuette, T.N. Ndou, A. Muñoz de la Peña, K.L. Greene, C.K. Williamson, I.M. Warner, J. Phys. Chem. 95 (1991) 4897.
[14] P. Rodriguez, M. Sanchez, J.R. Isasi, G. Gonzalez-Gaitano, Appl. Spectrosc. 56 (2002) 1490.
[15] M. Panda, A.K. Mishra, J. Photosci. 9 (2002) 75.
[16] (a) H. Kobashi, M. Takahashi, Y. Maramatsu, T. Morita, Bull. Chem. Soc. Jpn. 54 (1981) 2815;
(b) G. Nelson, I.M. Warner, J. Phys. Chem. 94 (1990) 576;
(c) A. De Korte, R. Langlois, C.R. Cantor, Biopolymers 19 (1980) 1281.
[17] H. Shizuka, M. Fukushima, T. Fuju, T. Kobayashi, H. Ohtani, M. Hoshino, Bull. Chem. Soc. Jpn. 58 (1985) 2107.
[18] T. Yorozu, M. Hoshino, M. Imamura, J. Phys. Chem. 86 (1982) 4422.
[19] N. Chattopadhyay, T. Chakraborty, A. Nag, M. Chowdhury, J. Photchem. Photobiol. A 52 (1990) 199.
[20] (a) S. Hamai, J. Mat. Chem. 15 (2005) 2881;
(b) L. García-Río, P. Hervés, J.R. Leis, J.C. Mejuto, J. Pérez-Juste, P. Rodriguez-Dafonte, Org. Biomol. Chem. 4 (2006) 1036;
(c) L. Viola, R.H. de Rossi, Can. J. Chem. 77 (1999) 860.
[21] R.L. Van Etten, G.A. Clowes, J. Am. Chem. Soc. 89 (1967) 3253.
[22] C. Sanramé, R.H. de Rossi, G. Argüello, J. Phys. Chem. 100 (1996) 8151.
[23] R.W. Cowgill, Biochim. Biophys. Acta 133 (1967) 6.
[24] S. Tobita, H. Shizuka, Chem. Phys. Lett. 75 (1980) 140.
[25] (a) T. Förster, Chem. Phys. Lett. 17 (1972) 309;
(b) Z.R. Grabowski, W. Rubaszewska, J. Chem. Soc., Faraday Trans. I 73 (1977) 11;
(c) B. Marciniak, H. Kozubek, S. Paszyc, J. Chem. Educ. 69 (1992) 247.
[26] K.A. Connors, Binding Constants, John Wiley and Sons, New York, USA, 1987.
[27] A. Örstan, J.B. Ross, J. Phys. Chem. 91 (1987) 2739.
[28] (a) R.E. Galian, A.G. Bracamonte, A.V. Veglia, Anal. Chim. Acta 540 (2005) 393;
(b) R. Galian, A. Veglia, R.H. de Rossi, Analyst 123 (1998) 1587;
(c) R. Galian, A. Veglia, R.H. de Rossi, Analyst 125 (2001) 1465.
[29] D. Carićí, V. Tomišić, M. Kveder, N. Galić, G. Pifat, V. Magnus, M. Šoškić, Biophys. Chem. 111 (2004) 247.
[30] N. Chattopadhyay, A. Samanta, T. Kundu, M. Chowdhury, J. Photochem. Photobiol. A 48 (1989) 61.
[31] N. Chattopadhyay, J. Photchem. Photobiol. A 58 (1991) 31.
[32] (a) N. Berova, K. Nakanishi, R. Woody, Circular Dichroism, Principles and Applications, 2nd ed., Wiley/VCH, USA, 2000, p. 480;
(b) N. Berova, K. Nakanishi, R. Woody, Circular Dichroism, Principles and Applications, 2nd ed., Wiley/VCH, USA, 2000, p. 743;
(c) N. Berova, K. Nakanishi, R. Woody, Circular Dichroism, Principles and Applications, 2nd ed., Wiley/VCH, USA, 2000, p. 827.